Accepted Article

Semi-Automatic Outlining of Levator Hiatus

Nikhil SINDHWANI[1,2] , Daniel BARBOSA[3], Martino ALESSANDRINI[3], Brecht HEYDE[3], Hans P. DIETZ[4], Jan D'HOOGE[3] and Jan DEPREST[1,2]

[1] Department of Development and Regeneration, Cluster Organ Systems, Biomedical Sciences, KU Leuven, and Obstetrics and Gynaecology, University Hospitals Leuven, Leuven, Belgium; [2]Interdepartmental Center for Surgical Technologies, Faculty of Medicine, KU Leuven, Leuven, Belgium; [3]Laboratory on Cardiovascular Imaging and Dynamics, Department of Cardiovascular Sciences, Faculty of Medicine, KU Leuven, Leuven, Belgium; [4]Sydney Medical School Nepean, Nepean Hospital, Penrith, Australia

Correspondence to: Dr J. Deprest, Department of Development and Regeneration & Centre for Surgical Technologies, Faculty of Medicine, KU Leuven, Leuven, 3000, Belgium (e-mail: Jan.Deprest@uzleuven.be)

Disclosures: HP Dietz has received unrestricted educational grants from GE Medical. JDh has joint research projects with GE Vingmed ultrasound and with Philips Healthcare.

Acknowledgements: JDe is a fundamental clinical researcher for the Fonds Wetenschappelijk Onderzoek Vlaanderen (1801207). NS receives a doctoral grant in the Bip-Upy project (NMP3-LA-2012-310389; FP7) funded by the European Commission.

This article has been accepted for publication and undergone full peer review but has not been through the copyediting, typesetting, pagination and proofreading process, which may lead to differences between this version and the Version of Record. Please cite this article as doi: 10.1002/uog.15777

This article is protected by copyright. All rights reserved.

Accepted Article

Abstract

Objective:

Our objective was to create a semi-automated levator hiatus outlining tool to reduce inter-observer variability and speed up analysis.

Methods:

The proposed Automated Hiatus Segmentation algorithm (AHS) takes a C-plane image (image in the plane of minimal hiatal dimensions) and the vertical hiatal limits as inputs. The AHS then creates an initial outline by fitting pre-defined templates on an intensity invariant edge map which is further refined using the B-spline active surfaces framework.

The AHS was tested using 91 representative C-plane images. Reference hiatal outlines were obtained manually and compared to the AHS outlines by three independent observers. The Mean Absolute Distance (MAD), Hausdorff distance, Dice and Jaccard Coefficients were used to quantify segmentation accuracy. Each of these metrics was calculated both for Computer-Observer Differences (COD) and Inter-Observer Difference. The Williams Index was used to test the null hypothesis that the automated method agrees with the operators at least as well as the operators agree with each other. Agreement between the two methods was studied using the Intraclass Correlation Coefficient (ICC) and Bland-Altman plots.

Results:

The AHS contours matched well with the manual ones (COD = 2.10 (1.54) mm [Median (IQR)] for MAD). The WI was greater than or close to 1 for all quality metrics indicating that the algorithm performs at least as well as the manual referees in terms of inter-rater variability. The IODs using each of the difference metrics were significantly lower when using the AHS. A higher ICC was achieved when using the AHS (0.93). The Bland Altman plots show negligible bias between two methods. Using the AHS took about 7.07(3.49) s compared to manual outlining that took 21.31(5.43)s [Median(IQR)], thus achieving a speedup of almost 3X.On an average the hiatus could be outlined completely using only three points, two for initialization, with one for manual adjustment.

Conclusions:

We present for the first time a method for tracing hiatal outline with minimal user input. The AHS is fast, robust, reliable and improves inter-rater agreement.

This article is protected by copyright. All rights reserved.

Accepted Article

Introduction:

Pelvic organ prolapse is the abnormal herniation of pelvic organs through the genital hiatus. It is common, conveying a lifetime risk for a single surgery for all women between 10 and 20%[1,2]. It is widely accepted that weakening or failure of pelvic floor support structures (muscles, fascias and/or ligaments), directly causing prolapse. Ultrasound is the most widely used imaging modality to assess the anatomical integrity and function of pelvic floor. Besides it is also simple, safe and, affordable to use. Mobility of pelvic organs on Valsalva and the shape and size of the levator hiatus are measured during a routine examination[3]. The levator hiatus is particularly important as it is the largest potential hernia portal in the human body. The hiatal dimensions and its appearance have been correlated with severity of prolapse, levator muscle avulsion and even prolapse recurrence after surgery[4–6]. However, currently these measurements are done manually and only in certain specialized centers. Further, recent studies have expressed concerns about reliability and agreement between operators, particularly when diagnosing muscle trauma[7]. Smart algorithms of pattern recognition have the potential to significantly increase the acceptance and reliability of these measurements.

Development of automated segmentation algorithms for ultrasound images is challenging as the image quality may depend on acquisition parameters, tissue quality, and operator experience. Further, low signal-to-noise-ratio, presence of spurious speckle patterns, shadows etc. causes variations in appearance of a structure or even missing boundaries[8]. While automation or intelligent enhancements of ultrasound images have been explored widely for obstetric, prostate and cardiovascular applications, only a limited effort has been made in urogynaecology[9,10].

We present, for the first time, a semi-automatic methodology for outlining the genital hiatus with minimal user input. Currently in the clinic, the levator hiatus is outlined in the axial plane of minimal hiatal dimensions, or the C-plane. The C-plane is identified by marking the posterior aspect of Symphysis Pubis (SP) and the anterior border of Pubo-Visceral muscle (PVM)[4]. Next, the user manually traces the hiatal boundary to measure its area. Our method seeks to automate and/or simplify this latter tracing step.

Methods:

Algorithm

The segmentation pipeline was implemented in an interactive user interface in Matlab v2013a (Mathworks Inc., Natik, USA), henceforth referred to as the Automated Hiatus Segmentation tool or the AHS tool.

In the C-plane image, the hiatal outline is generally clearly visible, as the levator muscle is hyperechogenic compared to the locally hypoechogenic interior. However, it may vary greatly in shape and texture, depending on the presence of uni- or bilateral levator avulsion, and if the image was taken on rest, contraction or Valsalva.

The AHS utilizes a phase-based approach of edge detection, which is intensity invariant and has been successfully used in echocardiography[8,11–14]. Further, a gradient directionality condition removes all spurious edges, and keeps only those that may represent the interior boundary of the levator muscle, to give us the edge map *E*. Next, we match several simple pre-defined templates so as to interpolate over any missing boundaries in the image. The template matching step is repeated on

This article is protected by copyright. All rights reserved.

Accepted Article

either side (right and left) of the SP-PVM line to capture any asymmetric anatomical variations. Finally, a level set methodology refines the initial contour using the B-spline Explicit Active Surfaces (BEAS) framework, introduced for cardiac segmentation by Barbosa et al[15]. Additionally, an optional interactive adjustment step is implemented to manually refine the segmentation result in real time. The number of points needed to adjust the segmentation is also recorded. An overview of the AHS is given in Table 1.

The following section describes the AHS algorithm in detail.

1. Preprocessing

In practice, it is common to use a volume rendered image to enhance visualization of anatomical structures[3]. A grayscale based volume rendering is used by merging 11 gamma corrected ($\gamma = 2$) image planes, 5 above and 5 below parallel to the C-plane[16].

2. Get monogenic edge map

The monogenic signal of the image is used to detect step edges using the feature asymmetry (FA) measure as proposed by Rajpoot *et al* [12], following the original concepts introduced in Mulet-Prada *et al* [17]. The FA has values in the range [0, 1], close to zero in homogeneous regions and close to one near edges[11]. A threshold of 0.4 was empirically determined to represent a significant edge for our case and was used to binarize the FA map. Figure 1(A-C) shows the original axial ultrasound image in the C-plane, I, the corresponding FA signal, I_{FA}, and the edge map obtained after thresholding, I_{FA}^{bw}.

The FA image detects many spurious edges and thus needs to be filtered. A first step is the selection of the region of interest (ROI). The ROI is defined as the region inside a 5px border, above and below the SP and PVM points between the image acquisition boundaries, represented by the red border in Figure 1(D). Further filtering will be performed taking into account the anatomical appearance of hiatal boundary, explained next.

In Figure 1(A), one can see that the interior of the hiatus is locally hypo echogenic compared to the surrounding hyper echogenic levator muscle[4]. We can use this to further filter the monogenic edge map. Indeed, the gradient direction of points belonging to the hiatal outline should point towards the middle of the hiatus. Using this *gradient directionality criterion,* we can therefore move all points where the gradient points away from the hiatal mid.

To achieve this the binarized FA signal is skeletonized and the directionality of the edges, as indicated by the monogenic signal, is evaluated at each pixel belonging to this skeleton, see Figure 1(E-F). Pixels from this skeleton corresponding to the above gradient directionality criterion then survive, as shown in Figure 1(G). Finally, the edge map *E* is obtained by separating a neighborhood around all surviving pixels on the original FA signal (Figure 1(H)).

3. Template Matching

For images where the hiatal boundary is clearly visible, the edge map *E* usually represents a good approximation of the hiatus. However, this is not always the case due to missing or unclear boundaries. Thus, a series of pear shaped curves are used as templates for finding the best initial left

This article is protected by copyright. All rights reserved.

Accepted Article

resp. right hiatal contour. Eq.1 is the Cartesian equation for the Mandelbrot set lemniscate L_3, which, for some range of r, appears like a pear-shaped curve [18].

$$r^2 = (x^2 + y^2)\left(\begin{array}{c} 1 + 2x + 5x^2 + 6x^3 + 6x^4 + 4x^5 + x^6 + \\ -3y^2 - 2xy^2 + 8x^2y^2 + 8x^3y^2 + 8x^4y^2 + \\ 2y^4 + 4xy^4 + 5x^2y^4 + 5x^3y^2 + y^6 \end{array}\right) \quad \text{Eq.1}$$

where, *r* takes discrete values of 0.8, 1, 1.5, 3, 5 and 7 to generate different shapes of the pear curve Figure 3. The values of *r* are chosen to represent the likely shapes of the hiatal outline.

Each vertical axis of each template is aligned along the SP-PVM line to localize the templates. The templates are further scaled along the horizontal axis to obtain 6 curves for each value of *r*, with aspect ratios 0.5, 0.62, 0.74, 0.86, 0.98 and 1.1. The values were chosen empirically to span the range of likely shapes. Thus a set of 36 template curves, T are obtained. Figure 2(A) shows some of the template curves superimposed on the monogenic signal.

To find the template that best matches the hiatal outline, we use the classical template matching approach. This approach calculates the overlap score of the template curves with the edge map. If $S_t = \sum_{x,y}(I_t(x,y) \cdot E(x,y))$, is the overlap score, where $I_t(x,y)$ is the template image with a value of 1 in a 10 pixel neighborhood of the template curve and 0 otherwise; then the ideal template t^* would be such that $S_{t^*} = \max_{t \in T} S_t$.

It is common to have asymmetric anatomical variations laterally, especially in cases where patients have a levator avulsion. Therefore, template matching is done separately on the right and left hand sides of the hiatus. The middle point of the SP-PVM points defined by the user divides the hiatus laterally into right and left sides. The resulting template curves are then merged on their corresponding side to obtain the initial approximation of hiatal boundary. An example is illustrated in Figure 2(B).

4. Refine initial approximation using BEAS

Further refinement of the initial approximation is done by running a 2D version of B-spline Explicit Active Surface (BEAS) on the original image[15]. The fundamental concept of this method is to regard the boundary of an object as an explicit function, where one of the coordinates of the points within the surface is given explicitly from the remaining coordinates. For the case of a 2D closed object, the boundary can be represented in the polar space, thus the contour radius is being represented as an explicit function of the angle. The refinement can thus be expressed as an optimization problem. Using a B-spline representation of this explicit function, BEAS obtains a contour representation that can be driven towards certain image characteristics in a computationally efficient manner. In this work, the image feature was the difference between the gray levels inside and outside the hiatal area (i.e. the contour). Further details on this segmentation formalism can be found in Barbosa et al., 2012, and Barbosa et al., 2013[15,19].

Figure 2(C.1) shows the first step after the initialization. The initial contour found after template matching is shown in red with direction of evolution shown with cyan arrows. The final segmentation result after refinement is shown in Figure 2(C.2).

This article is protected by copyright. All rights reserved.

Accepted Article

5. Manual Adjustment of hiatus segmentation

If the resulting segmentation is not to the user's satisfaction, (s)he can steer the segmentation by interactive adjustment of the contour by clicking on the pixel where they think the contour should pass through. The underlying mathematical formalism for such interactive real-time adjustment has been described previously[20]. The number of points needed for adjustment was recorded.

Test Data

To get as close to the clinical situation as possible, we first used de-identified transperineal ultrasounds from 20 consecutive women that had symptoms of pelvic floor dysfunction obtained at a tertiary urogynaecological clinic in Penrith, Australia, between May-June 2014. The ultrasound volumes from this dataset record all three states of the levator muscle that are routinely examined, namely, rest, contraction and full valsalva. C-plane images showing the levator hiatus in all these three states were extracted according to established protocols[21].

Secondly, to test the performance of the AHS tool on a wider range of anatomical variability, 15 de-identified 4D volumes and one 3D volume publically available with the educational Atlas of Pelvic Floor Ultrasound were used[3]. In these 15 4D volumes, only the Valsalva maneuver was imaged and thus, C-plane images only at rest and full Valsalva were extracted. Detailed patient information is included for reference in Appendix A.

Thus, from ultrasound volumes of 36 patients, a total of 91 C-plane images were selected, 35 images at full Valsalva, 36 at rest and 20 at contraction. The C-planes images used here were pre-selected by a single operator (NS). NS had previously passed a test-retest series for manual outlining using standardized protocols [22]. This pre-selection was done in order to test the performance of AHS for its primary purpose, i.e., accurate outlining of the hiatal boundary on a 2D C-plane image. Such pre-selection was also necessary for quantitative evaluation of hiatal outlines generated by AHS with both contour and region based metrics as described in the next section, which gave us a much more comprehensive picture of AHS' performance.

Three operators, namely, NS, Dr. Ixora Tan (IT), and Dr. Friyan Tuyrel (FT), passed a test-retest series (data not shown) according to established methods[22]. They then performed hiatal outlining on the 91 images using the AHS tool and using manual outlining methods, one time each. At the time of this analysis they had 1 year, > 4 years and 6 months experience in acquiring and/or analyzing pelvic floor ultrasound volumes respectively. For practice, all three observers performed additional hiatal outlining using the AHS on 10 practice images, which were different from the 91 images used for analysis.

The median pixel size of the image was 0.5mm, range (0.40-0.65). All images were used for statistical analysis, regardless of their quality, or the appearance of pelvic floor structures.

Quantitative metrics for evaluation

Several metrics are proposed to describe the similarity of manual and computer generated outlines[23]. We chose the mean absolute distance (MAD) and the Hausdorff distance (HD), as two boundary based similarity metrics. Also, we calculated the Jaccard Coefficient and the DICE coefficient as two region based similarity metrics. A detailed description of these quantitative metrics is provided in

This article is protected by copyright. All rights reserved.

Accepted Article

Appendix B. We also compare the hiatal area output by the manual method with the one from the AHS method as it is a clinically important parameter.

Computer-Observer and Inter-Observer Differences

The computer-observer differences (COD) and inter-observer differences (IOD) were evaluated according to the guidelines provided by Chalana and Kim[24]. Briefly, CODs were evaluated by calculating all four similarity metrics between all possible combinations of computer generated and manually outlined curves (for each image there are 3 manual and 3 AHS contours, thus giving 9 difference measurements). Similarly, the Inter-Observer difference (IOD) was evaluated by calculating similarity metrics between curves manually generated by the three operators. The manually obtained contour from each observer is compared against the contour of two other observers, thus giving a total of 3 inter-observer difference measurements per image. Since the AHS requires initial placement of SP and PVM points and may require further manual adjustment, we calculated the inter observer differences for outlines obtained using the AHS tool as well, henceforth referenced as IOD_{AHS}. As before, IOD_{AHS} is also calculated for 3 difference measurements per image. An overall summary of COD, IOD and IOD_{AHS} is represented as median ± IQR in table 1. COD, IOD and IOD_{AHS} values were tested for statistical significance using student's t-test.

Willliams Index

To test the reliability of AHS, the modified Williams Index (WI) was calculated for each similarity metric. The WI is used to test the null hypothesis that the automated method agrees with the operators at least as well as the operators agree with each other (i.e., the method is within inter-observer variability range)[24]. In practice, whenever the upper bound of the 95% confidence interval (CI) of the WI is greater than one, there is no statistical evidence that the agreement between AHS and the manual references is worse than the inter-observer agreement.

Comparison of Hiatal Area measurements

To calculate any bias in hiatal area calculation when using AHS and manual outlining, we created Bland-Altman plots from all differences in area measurements between manual and AHS contours for each image (total 9 area difference values per image)[25]. Area measurements from manual contours were also compared to determine the inter-observer bias. In addition, the Intra-class Correlation Coefficient (ICC, single measurement, absolute agreement definition) was calculated between paired manual and AHS hiatal area measurements[22].

Results:

Table 2 shows a summary of the COD, IOD, IOD_AHS and WI (with 95% CI) using each of the difference metrics for the 91 images. The CODs were found to be statistically similar to IODs for all distance metrics, indicating that the AHS interprets the boundaries similar to any other observer. The IOD_{AHS} was found to be significantly lower ($p=0.005$ for HD and $p<0.001$ for all others) than the IODs. This indicates that when users use the AHS, their outlines are much more similar than when using manual methods.

Visually, the computer generated curves matched well with the manually generated outlines. Figure 3 (a-d) shows the results in order of quality according to the MAD metric. The images represent the

This article is protected by copyright. All rights reserved.

Accepted Article

0^{th}, 25^{th}, 50^{th} and 100^{th} percentile of average MAD values respectively. For qualitative assessment of the performance of the algorithm for different clinical cases, Figure 3 (e-h) show a case of normal levator anatomy, a ballooning hiatus, an unilateral avulsion, and that of a bilateral avulsion respectively.

When area measurements calculated from manual outlines of the three referees were compared for agreement, an ICC of 0.885 was noted. When looking at agreement between users when using the AHS method, the ICC was 0.932, higher than when using manual methods. The area measurements done using manual and AHS also agree well with an ICC of 0.91.

Hiatal area measurements done using the AHS method are on an average lower by 2.5 cm^2, as seen from Bland Altman analysis in Figure 4 (A). However, this mean bias is well within the range of inter-observer biases in area measurements done manually as shown in Figure 4(C-D).

The time taken to outline the hiatus using AHS was 7.07±3.49 seconds. The biggest portion of this time was taken up by initialization (4.88±2.23 sec), i.e., marking the SP and PVM points. The calculation run time was 1.68±0.25 seconds. Further adjustment was done interactively, and took 0.23±0.74 seconds. All values are presented as median ± IQR. The times were calculated on a standard notebook computer (ASUS Ultrabook, Intel® Core™i5-3537CPU@1.7GHz, 8GB RAM). Average time taken for manual contouring was 21.31±5.43 seconds.

In 252 out of 273 trials (92%) of all segmentations done with the AHS, it required three or less points to further adjust the contour. In about 73% trials (200 of 273), the AHS required one or no adjustment. Table 3 shows the complete breakdown of scores.

Discussion:

The AHS algorithm presented here is, to our knowledge, a first attempt to a computer assisted methodology to segment hiatal outline with minimal user input. We tested the AHS on a challenging dataset that encompasses both, a sequential series of patients and an extreme case scenario with images from a very wide range of anatomical variability. Even so, the algorithm performs very well. Quantitatively, for example, a COD of 2.1 mm for MAD, indicates that on an average, the AHS contours do not end up very far from what an experienced observer would have drawn. Further, the values of COD are similar or significantly lower than IOD for all tested metrics, indicating that the algorithm potentially improves the inter-rater variability. A WI of greater than or close to 1 further indicates that the algorithm performs at least as well as the manual referees in terms of inter-rater variability.

The findings from Bland-Altmans plots indicate the same, as the mean bias in area measurements when using AHS is within the range of the mean bias from manual contouring.

Finally, a higher ICC when measuring the hiatal area using AHS compared to manual outlining decidedly proves that using AHS improves the agreement between observers.

Besides being more accurate and reliable, there is also significant time savings when using AHS. It takes up to 3 times less time to outline the hiatus using AHS than when using outlining manually. This is because when using the AHS, the outline could be detected using only 3 points (range 2-7), instead of about 14 points (range 10-24) when outlining manually.

This article is protected by copyright. All rights reserved.

Accepted Article

One limitation of the current study design is that the algorithm needs to be initialized on axial images, and not on sagittal images where the plane of minimal hiatal dimensions is first identified. This can be easily remedied in a future implementation as the SP and PVM points defined on axial and sagittal images are usually the same. However, this was necessary in order to remove discrepancies that may arise due to different selection of the C-plane. Another limitation is that the AHS currently works in the MatLab environment and may potentially be less available to clinicians. Ideally, such a tool may be integrated to commercial software tools that are more familiar to the clinicians such as 4DView. We will explore this option in the future. Finally, the present study is not patient controlled, and as such does not provide any insight as to the performance of the algorithm in different clinical scenarios, such as in patients with avulsion, or a ballooning hiatus. Since we did not initially control for these scenarios, the current dataset does not have enough power to conclusively state one way or the other. Further studies will evaluate the algorithm with regards to these clinically important outcome measures.

A good 2D outlining of the hiatus opens possibilities of extending the analysis into 3 and 4 dimensions to provide a 3D/4D visualization of urogenital hiatus and further functionally assess the levator muscle. The AHS can easily be extended for automated assessment of levator avulsion as already proposed by Ismail et al.[26]

Conclusions:

We introduce for the first time, a robust automated approach to outline the genital hiatus. We used the existing BEAS framework that was previously successfully used in cardiology. The AHS tool is reliable and reduces inter-observer variability. Such tool may enable high-throughput, automated processing of large and/or multicenter studies looking at correlations of hiatal dimensions with pelvic floor disorders.

Acknowledgement:

We are grateful for the support of several clinicians for their input. Special thanks to researchers from University of Western Sydney, namely, Dr. Ixora Atan, and Dr. Friyan Tuyrel who performed the manual outlining and AHS initialization for this study.

References:

1. Olsen AL, Smith V J, Bergstrom JO, Colling JC, Clark AL. Epidemiology of surgically managed Pelvic Organ Prolapse and Urinary Incontinence. *Obstet Gynecol 1997;* **89 :** 520–506.

2. Smith FJ, Holman CDJ, Moorin RE, Tsokos N. Lifetime risk of undergoing surgery for pelvic organ prolapse. *Obstet Gynecol 2010;* **116 :** 1096–100.

3. Dietz HP, Hoyte L, Steensma AB. *Atlas of Pelvic Floor Ultrasound*. Springer-Verlag Limited: London, 2008.

4. Dietz HP, Shek C, Clarke B. Biometry of the pubovisceral muscle and levator hiatus by three-dimensional pelvic floor ultrasound. *Ultrasound Obstet Gynecol 2005;* **25 :** 580–5.

This article is protected by copyright. All rights reserved.

Accepted Article

5. Abdool Z, Shek KL & Dietz HP. The effect of levator avulsion on hiatal dimension and function. *Am J Obstet Gynecol 2009;* **201 :** 89.e1–e5.

6. Dietz HP, Chantarasorn V, Shek KL. Levator avulsion is a risk factor for cystocele recurrence. *Ultrasound Obstet Gynecol 2010;* **36 :** 76–80.

7. Van Veelen GA, Schweitzer KJ, van Delft K, Kluivers KB, Weemhoff M, van der Vaart CH . Diagnosing levator avulsions after first delivery by tomographic ultrasound: reliability between observers from different centers. *Int Urogynecol J 2014;* **25 :** 1501–1506.

8. Boukerroui D, Noble JA, Brady M. Feature Enhancement in Low Quality Images with Application to Echocardiography. In *Inf Process Med Imaging 17th Int Conf IPMI 2001 Davis CA USA, June 18–22, 2001 Proc,* Insana MF, Leahy RM (eds). Springer-Verlag Berlin Heidelberg: New York, 2001; 453–460.

9. Shao F, Ling KV, Ng WS, Wu RY. Prostate boundary detection from ultrasonographic images. *J Ultrasound Med 2003;* **22 :** 605–23.

10. Hodge AC, Fenster A, Downey DB, Ladak HM. Prostate boundary segmentation from ultrasound images using 2D active shape models: optimisation and extension to 3D. *Comput Methods Programs Biomed 2006;* **84 :** 99–113.

11. Belaid A, Boukerroui D, Maingourd Y, Lerallut JF. Phase-based level set segmentation of ultrasound images. *IEEE Trans Inf Technol Biomed 2011;* **15 :** 138–47.

12. Rajpoot K, Grau V, Noble JA. Local-Phase Based 3D Boundary Detection Using Monogenic Signal and its Application to Real-Time 3D Echocardiography Images. In *Biomed Imaging From Nano to Macro, 2009.* ISBI '09 IEEE Int Symp, 2009; 783–786.

13. Alessandrini M, Basarab A, Liebgott H, Bernard O. Myocardial Motion Estimation from Medical Images Using the Monogenic Signal To cite this version : Myocardial Motion Estimation from Medical Images Using the Monogenic Signal. *IEEE Trans Image Process 2013*; **22 :** 1084–1095.

14. Kovesi P. Image Features from Phase Congruency. *Videre J Comput Vis Res 1999;* **1 :** 1–27.

15. Barbosa D, Dietenbeck T, Schaerer J, D'hooge J, Friboulet D, Bernard O. B-Spline Explicit Active Surfaces : An Efficient Framework for Real-Time 3-D Region-Based Segmentation. *IEEE Trans image Process 2012;* **21 :** 241–251.

16. Gonzalez RC, Woods RE, Eddins SL. *Digital Image Processing Using Matlab*. McGraw Hill Education India, 2010.

17. Mulet-Parada M, Noble JA. 2D+T acoustic boundary detection in echocardiography. *Med Image Anal 2000;* **4 :** 21–30.

18. Mandelbrot BB. *The Fractal Geometry of Nature*. W. H. Freeman and Company, 2010.

19. Barbosa D, Dietenbeck T, Heyde B, Houle H, Friboulet D, D'hooge J, Bernard O. Fast and fully automatic 3-d echocardiographic segmentation using B-spline explicit active surfaces: feasibility study and validation in a clinical setting. *Ultrasound Med Biol 2013;* **39 :** 89–101.

This article is protected by copyright. All rights reserved.

Accepted Article

20. Barbosa D, Heyde B, Cikes M, Dietenbeck T, Claus P, Friboulet D, Bernard O, D'hooge J. Real-time 3D interactive segmentation of echocardiographic data through user-based deformation of B-spline explicit active surfaces. *Comput Med Imaging Graph 2014;* **38 :** 57–67.

21. Dietz HP. Pelvic floor ultrasound in prolapse: what's in it for the surgeon? *Int Urogynecol J; 2011;* **22 :** 1221–32.

22. Brækken IH, Majida M, Ellstrøm-Engh M, Dietz HP, Umek W, Bø K. Test-Retest and intra-observer repeatability of two-, three- and four-dimensional perineal ultrasound of pelvic floor muscle anatomy and function. *Int Urogynecol J Pelvic Floor Dysfunct 2008;* **19 :** 227–235.

23. Huang Q, Dom B. Quantitative methods of evaluating image segmentation. In *Proceedings. Int Conf Image Process 1995.* 53–56.

24. Chalana V, Kim Y. A methodology for evaluation of boundary detection algorithms on medical images. *IEEE Trans Med Imaging* 1997; **16 :** 642–52.

25. Bland JM, Altman DG. Statistical methods for assessing agreement between two methods of clinical measurement. *Int J Nurs Stud 2010;* **47 :** 931–936.

26. Ismail SIMF, Shek KL, Dietz HP. Unilateral coronal diameters of the levator hiatus: baseline data for the automated detection of avulsion of the levator ani muscle. *Ultrasound Obstet Gynecol 2010;* **36 :** 375–378.

This article is protected by copyright. All rights reserved.

Accepted Article

Figure Legends:

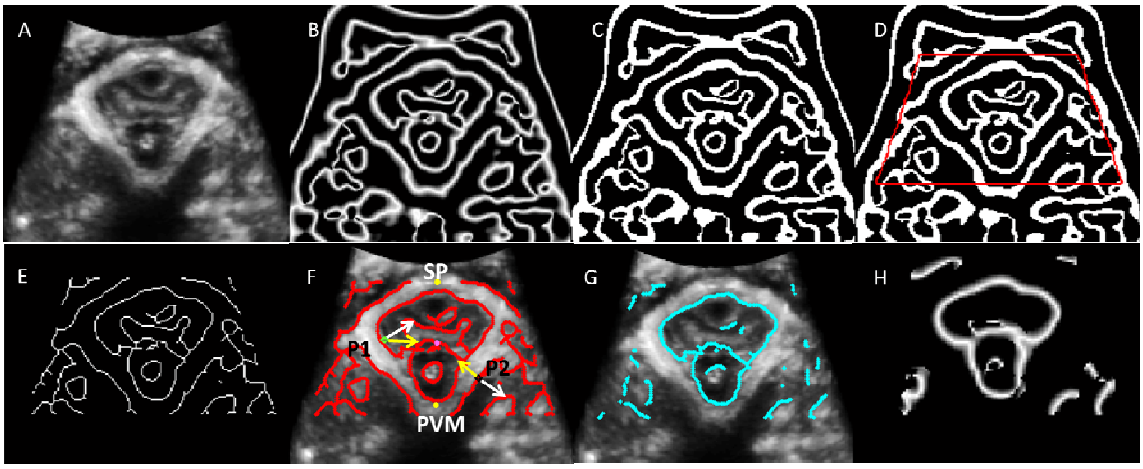

Figure 1: (A) the C-plane image, I. (B) is the corresponding FA signal, I_{FA}, (C) is the edge map obtained after thresholding, I_{FA}^{bw}. The red box in (D) shows the mask applied. Next, the binarized FA signal is skeletonized (E). All pixels belonging to this edge skeleton are then tested against the gradient directionality condition, (F). Two example points (black and green) lie on the edge skeleton. The vector from these points directed towards the hiatal middle (pink point) is shown with yellow arrow. The direction of the gradient at that pixel is shown in white. After removing all points that do not satisfy the gradient directionality condition, only a few pixels survive, shown in cyan in (G). The resulting edge map *E* is thus obtained by isolating a fixed neighborhood in the FA signal, (H).

This article is protected by copyright. All rights reserved.

Accepted Article

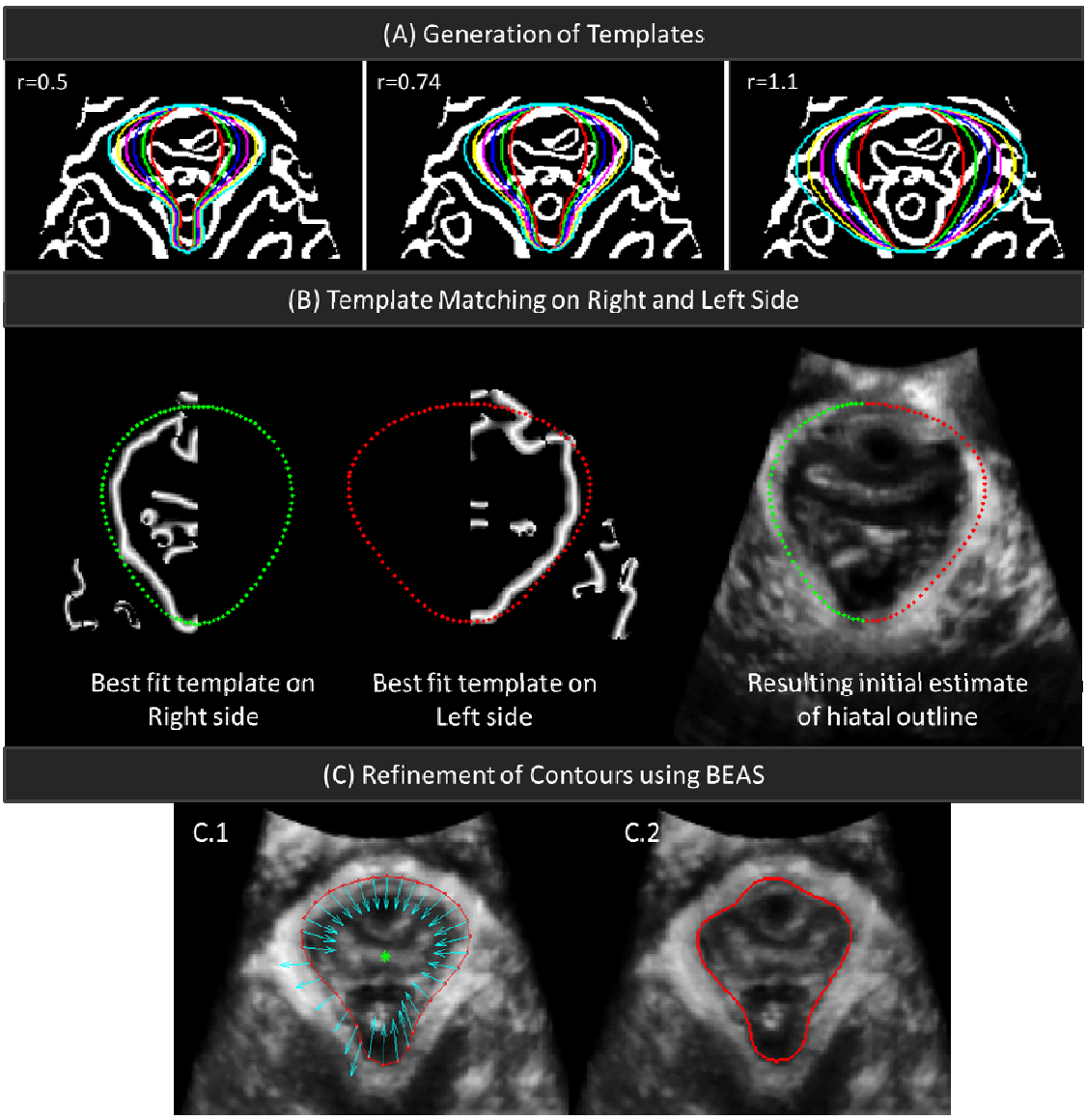

Figure 2: (A) Pear shaped curves obtained by using varying range value in the Cartesian equation of the Mandelbrot set lemniscate L3 are obtained. Some example template curves out of a total of 36 curves are shown. The red, green, blue, magenta, yellow and cyan curves represent curves of aspect ratios 0.5, 0.62, 0.74, 0.86, 0.98 and 1.1 respectively. (B)Template matching is done separately on the left and right sides of the hiatus and then merged to obtain the initial estimate of hiatus outline. (C) shows the contour refinement step using BEAS. After the best fit template contours (red) are found, the template is refined using BEAS. Cyan arrows (unscaled) in C.1 show the direction in which the contour points evolve. C.2 shows the hiatal outline contour in red after refinement using BEAS.

This article is protected by copyright. All rights reserved.

Accepted Article

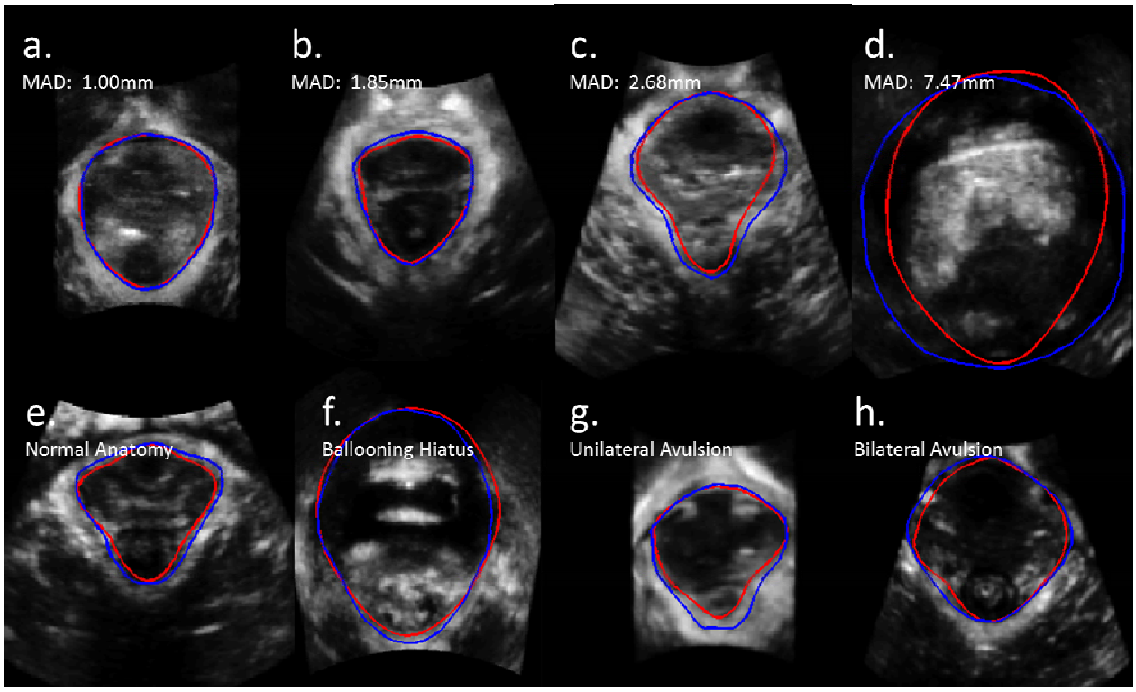

Figure 3: Results of the AHS algorithm compared to manual outlining. The averaged AHS contours are represented in red and the manual contours are represented in blue. The images **a** to **d** show a gradual decrease in quality such that they represent the 0^{th}, 25^{th}, 50^{th}, and 100^{th} percentile of the MAD respectively. Images **e** to **h** show a case of normal levator anatomy, a ballooning hiatus, an unilateral avulsion, and that of a bilateral avulsion respectively.

This article is protected by copyright. All rights reserved.

Accepted Article

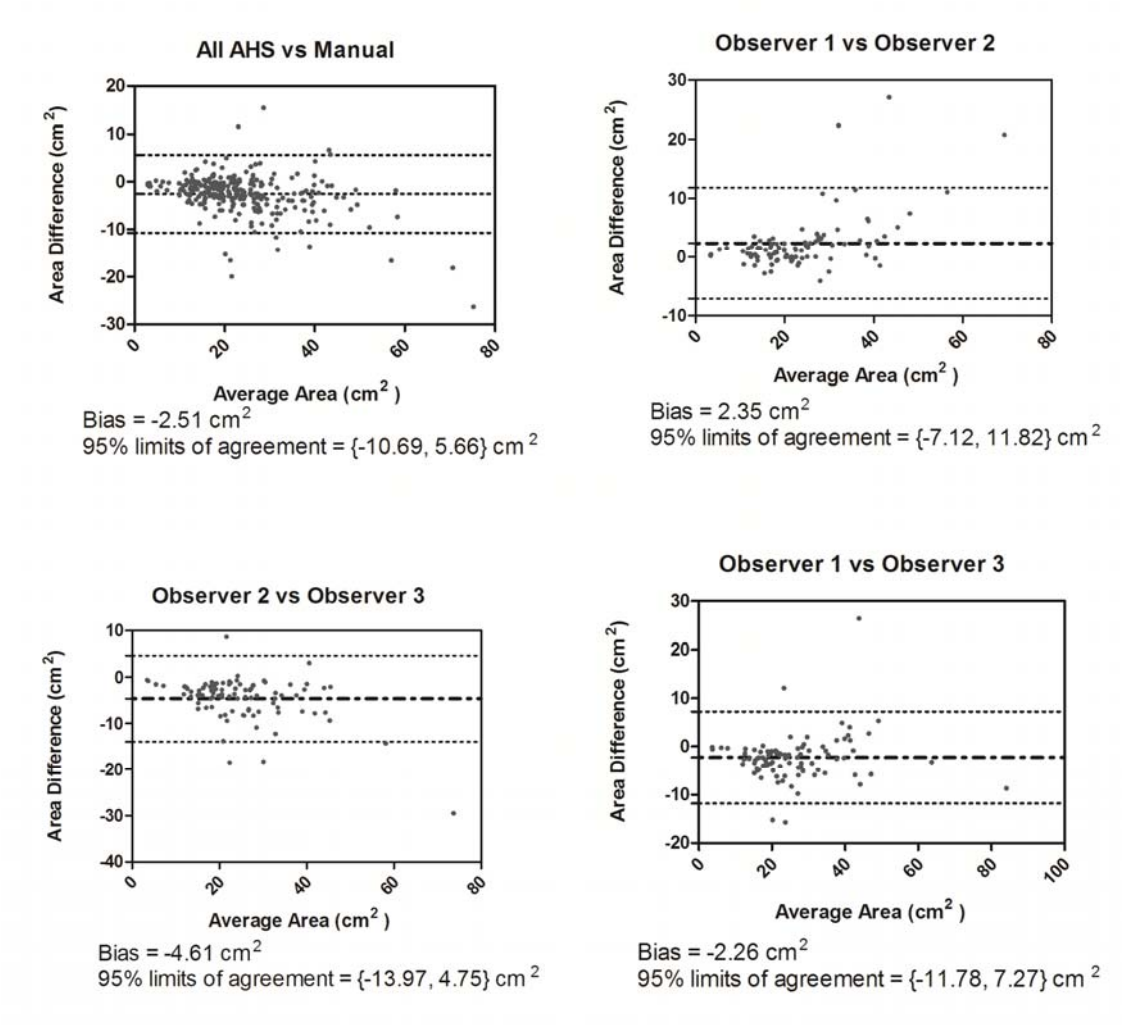

Figure 4: Bland Altman plots comparing measurements of hiatal area when made using AHS and when made manually is shown in (A). When comparing manually measured hiatal areas from observer 1 and observer 2, those of observer 2 and observer 3, and from observer 1 and observer 3 are shown in (B), (C) and (D) respectively.

This article is protected by copyright. All rights reserved.

Accepted Article

Table legends:

Table 1: Overview of Automatic Hiatus Segmentation (AHS) Algorithm

Table 2: Results of mean Computer Observer Differences (COD), Inter-Observer Differences (IOD) for the manual method, the IOD for the automatic method (IOD_{AHS}), presented as median ± IQR and the Williams Index along with its 95% CI. The results are presented for N=91 images.

Table 3: Frequency of points required for adjusting the AHS output

This article is protected by copyright. All rights reserved.

Accepted Article

Tables:

Table 1: Overview of Automatic Hiatus Segmentation (AHS) Algorithm

Input: 1. C-plane ultrasound Image. 2. User defined points SP and PVM on the C-plane image.
Output: Hiatal outline
Procedure: 1. Image Preprocessing. 2. Obtain the Edge map *E*. 2.1. Get feature anisotropy (FA) signal and binaries using threshold = 0.4 2.2. Filter FA image according to gradient directionality condition 3. Perform Template Matching 3.1. Create template images based on SP-PVM dimensions 3.2. Perform template matching on Right side 3.3. Perform template matching on Left side 3.4. Merge Right and left sides to obtain Initial estimated outline 4. Refine initial estimate using BEAS 5. Manual adjustment in real time if needed.

This article is protected by copyright. All rights reserved.

Accepted Article

Table 2: Results of mean Computer Observer Differences (COD), Inter-Observer Differences (IOD) for the manual method, the IOD for the automatic method (IOD_{AHS}), presented as median ± IQR and the Williams Index along with its 95% CI. The results are presented for N=91 images.

Parameter	COD (mm)	IOD (mm)	IOD_{AHS} (mm)	Williams Index	95% CI
Hausdorff Distance	5.73±3.90	6.02±4.43	5.22±5.02*	1.094	{1.087 1.101}
Mean Average Distance	2.10±1.54	2.2±1.43	1.80±1.42*†	1.093	{1.085 1.101}
Jaccard coefficient	0.85±0.09	0.85±0.10	0.88±0.10*†	0.995	{0.993 0.996}
DICE coefficient	0.92±0.05	0.92±0.06	0.93±0.06*†	0.996	{0.995 0.997}

* Statistically significant differences were found between IOD and IOD_{AHS} values for all quality metrics ($p = 0.005$ for HD and $p<0.001$ for others).

† The IOD_{AHS} values were statistically different from COD values for MAD metric, Jaccard and Dice metrics ($p<0.001$)

This article is protected by copyright. All rights reserved.

Accepted Article

Table 3: Frequency of points required for adjusting the AHS output

Additional points	Number of Images	Number of Images (%)	Number of images-cumulative % values
0	104	38.09524	38.09524
1	96	35.16484	73.26007
2	33	12.08791	85.34799
3	19	6.959707	92.30769
4	11	4.029304	96.337
5	6	2.197802	98.5348
6	2	0.732601	99.2674
7	2	0.732601	100

This article is protected by copyright. All rights reserved.